Research Article

Growth associated protein 43 and neurofilament immunolabeling in the transected lumbar spinal cord of lizard indicates limited axonal regeneration

https://doi.org/10.4103/1673-5374.324850

Date of submission: August 25, 2020

Date of decision: December 6, 2020

Date of acceptance: June 9, 2021

Date of web publication: September 17, 2021

Lorenzo Alibardi*

Graphical Abstract *Immunolocalization of GAP43 in regenerating axons of the injured lumbar spinal cord of lizard*

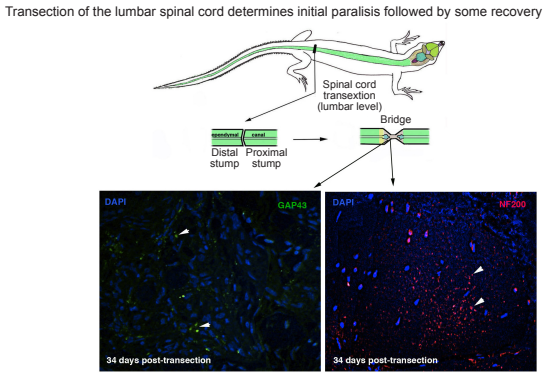

Immunolabeling for GAP43 and for NF200 shows axonal regeneration through the bridge

Abstract

Previous cytological studies on the transected lumbar spinal cord of lizards have shown the presence of differentiating glial cells, few neurons and axons in the bridge region between the proximal and distal stumps of the spinal cord in some cases. A limited number of axons (20–50) can cross the bridge and re-connect the caudal stump of the spinal cord with small neurons located in the rostral stump of the spinal cord. This axonal regeneration appears to be related to the recovery of hind-limb movements after initial paralysis. The present study extends previous studies and shows that after transection of the lumbar spinal cord in lizards, a glial-connective tissue bridge that reconnects the rostral and caudal stumps of the interrupted spinal cord is formed at 11–34 days post-injury. Following an initial paralysis some recovery of hindlimb movements occurs within 1–3 months post-injury. Immunohistochemical and ultrastructural analysis for a growth associated protein 43 (GAP-43) of 48–50 kDa shows that sparse GAP-43 positive axons are present in the proximal stump of the spinal cord but their number decreased in the bridge at 11–34 days post-transection. Few immunolabeled axons with a neurofilament protein of 200–220 kDa were seen in the bridge at 11–22 days post-transection but their number increased at 34 days and 3 months post-amputation in lizards that have recovered some hindlimb movements. Numerous neurons in the rostral and caudal stumps of the spinal cord were also labeled for GAP43, a cytoplasmic protein that is trans-located into their axonal growth cones. This indicates that GAP-43 biosynthesis is related to axonal regeneration and sprouting from neurons that were damaged by the transection. Taken together, previous studies that utilized tract-tracing technique to label the present observations confirm that a limited axonal re-connection of the transected spinal cord occurs 1–3 months post-injury in lizards. The few regenerating-sprouting axons within the bridge reconnect the caudal with the rostral stumps of the spinal cord, and likely contribute to activate the neural circuits that sustain the limited but important recovery of hind-limb movements after initial paralysis. The surgical procedures utilized in the study followed the regulations on animal care and experimental procedures under the Italian Guidelines (art. 5, DL 116/92).

Key Words: GAP-43; immunocytochemistry; lizard; neurofilaments; regeneration; spinal cord

Chinese Library Classification No. R446; R741; Q2

Introduction

Total or partial transection or crushing of the lumbar spinal cord (SC) in mammals and birds determines a permanent paralysis in the hindlimbs and impairment of motor and sensory abilities, depending on the extension of the injury (Chernoff, 1996; Tanaka and Ferretti, 2009; McDonough and Martinez-Cerdeno, 2012; Zhang et al., 2012; Lee-Liu et al., 2013). Generally, no axons can cross the discontinuity formed between the rostral (proximal) and the caudal (distal) SC stumps where a glial scar is formed. Some recovery is however possible in embryonic stages in birds and mammals (Clearwaters, 1954; Steeves et al., 1994), or even in relatively immature marsupials (Nicholls and Saunders, 1996; Martin et al., 2000). This suggests that in adult endotherms, where it is essential to maintain neural circuits fixed for performing complex sensory-motor coordinated movements, neural plasticity may be incompatible. The sophisticated adaptive immune system of the vertebrates is one of the main factors that lead to failure SC and neural regeneration in amniotes (Berry and Ritches, 1974; Lauro et al., 1992; Lennon, 1994; Gadani et al., 2015; Mescher et al., 2016).

Compared with amniotes, numerous anamniotes

Comparative Histolab Padova and Department of Biology, University of Bologna, Bologna, Italy

*Correspondence to: Lorenzo Alibardi, PhD, lorenzo. alibardi@unibo.it.

https://orcid.org/0000-0002-8247-2217 (Lorenzo Alibardi)

How to cite this article: *Alibardi L (2022) Growth associated protein 43 and neurofilament immunolabeling in the transected lumbar spinal cord of lizard indicates limited axonal regeneration. Neural Regen Res 17(5):1034-1041.*

(cyclostomes, cartilaginous and bony fish, urodele amphibians and anuran tadpoles) have a lower nerve complexity and can better recover a broad functionality and part of the original anatomy of the SC after an initial paralysis following SC injury (SCI) (Filoni et al., 1984; Chernoff, 1996; Ferretti et al., 2003; Tanaka and Ferretti, 2009; Lee-Liu et al., 2013; Rasmussen and Sagasti, 2016). SC regeneration in reptiles, ectotherm amniotes that occupy an intermediate position between anamniotes and endotherm amniotes, remains open to further comparative analysis on their ability to regenerate axons after injury. The comparative study is aimed to detect the key mechanisms and molecules that in lizards but not in mammals are evoked from the injury. This information is important to understand the reasons for the failure of SC regeneration in endotherm amniotes such as birds and mammals. No reports are available, to the best of our knowledge about SC recovery after lesion in crocodilians and snakes. Few researches on lizards (Raffaelli and Palladini, 1969; Srivastava, 1992; Srivastava et al., 1994; Alibardi, 2014a, b, c) and turtles (Reherman et al., 2009, 2011) have shown that after lumbar or thoracic SC injury or transection, these reptiles can partially recover a partial functionality. Following an initial paralysis, a good recovery of the hindlimb mobility returns after about 1 month in turtles (Rehermann et al., 2011). Also in lizards the complete or partial transection of the lumbar SC determines an initial paralysis of hindlimb movements. However, in a variable but significant number of lizards, a functional recovery starts after 3–4 weeks from the trauma (Raffaelli and Palladini, 1969; Srivastava, 1992; Srivastava et al., 1994; Alibardi, 2014a, b, c). A constant observation is that, within 3 months post-injury, recovery varies from lizards showing little capability to use the hindlimbs for stepping to lizards that perform similar movements as before the trauma. However, the original strength in the hindlimbs is not well recovered and the hind-limbs appear not capable to sprint and lift the body of these injured lizards above the ground. The knowledge of the cellular mechanisms behind the important functional recovery would be useful to understand the complete failure of SC regeneration in mammals and guide possible medical intervention to improve SC recovery in humans.

Previous cytological studies on the transected lumbar SC of lizards have shown the presence of differentiating glial cells, few neurons and axons in the bridge region. The bridge region is a 1–2 mm long region located between the proximal and distal stumps of the injured spinal cord segment in some cases (Alibardi, 2014b, c, 2019a; **Figure 1**).

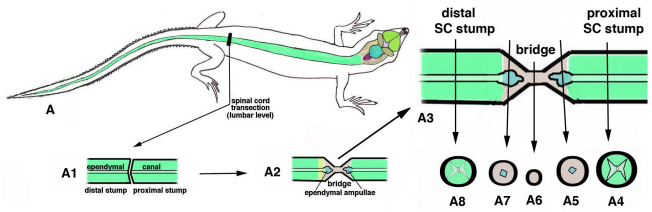

Figure 1 | **Self-explanatory schematic drawing indicating the point of spinal cord (SC) injury (A), the formation of a gap (A1) and of the following bridge (A2). A3 provides information on the indicative areas analyzed in the present study, as represented in cross-sections from rostral (proximal) to caudal (distal) SC spanning across the lesion. A4–A8 are the cross sections at the levels indicated by the arrows.**

A limited number of axons (20–50) can cross the bridge region and re-connect the caudal SC stump with small neurons located in the rostral stump of the SC. This axonal regeneration appears to be related to the recovery of hind limb movements after the initial paralysis, but further evidence for axonal regeneration is needed. The present study extends previous observations and shows that during the initial 2–4 weeks up to 3 months post-trauma, growth associated protein 43 (or neuromodulin), a useful marker indicating axonal growth also in lizards (Rodger et al., 2001), is detectable in some axons and numerous neurofilament-200 positive axons are also seen in the bridge. Few axons can even cross the entire bridge region and make connections between the rostral and caudal stumps of the SC. The present qualitative immunohistochemical observations support previous findings showing that a limited nervous connection occurs in the bridge region of the injured lumbar SC in some lizards, reconnecting the two sides of the interrupted SC and sustaining the functional recovery of limb movements.

Materials and Methods

Experiments and sample preparation

The preparation and embedding of the tissues utilized in the present study were conducted on adult individuals of the wall lizard (*Podarcis muralis*), as previously reported (Alibardi, 2019a). Briefly, adult lizards of both sexes were utilized, and the surgical procedures utilized in the study followed the regulations on animal care and experimental procedures under the Italian Guidelines (art. 5, DL 116/92). The lizards were anesthetized with ethylic ether and the skin with the dorsal and inter-vertebral muscles were sectioned to uncover the lumbar vertebral column. Using a sharp scissor, an incision was made between the 3rd or the 4th lumbar vertebra from the pelvic girdle to transect the exposed SC. The tail characteristically begun to wiggle for 1–2 minutes, and bleeding from the transected SC was blotted with clean paper and rapidly stopped. After checking the transection of the SC, vertebrae were re-aligned and the severed dorsal muscles were recomposed over the vertebrae. The skin borders were pulled over the incision by fine tweezers to cover as much as possible the muscle tissues. No suture was made to close the skin, and the skin borders were left to cover the incision in addition to the blood clot. The latter was impregnated with Cicatrene antibiotic powder (Welcome Italia, Pomezia-Rome, Italy) so that the blood-Cicatrene mixture rapidly coagulated over the incision. Eleven operated lizards were utilized after 11 (n = 3), 19 (n = 2), 22 (n = 3), and 34 (n = 3) days post-injury. Other three operated lizards were kept for 3 months after injury before being sacrificed and the vertebral column was collected in the operated region.

The injured SC, still enclosed in the excised vertebral column (about 2 vertebrae above and 2 vertebrae below the operated level of transection), was immediately immersed in the fixative (4% paraformaldehyde in Phosphate buffer 0.1 M at pH 7.4) at 4°C. After about 5 minutes, the vertebrae kept immersed in the fixative were delicately cut open under a stereomicroscope using tweezers and a fine scissor was used to remove the bone tissue and allow the rapid penetration of the fixative into the SC. Fixation of the SC mostly free from bones lasted about 8 hours at 4°C. The SC with the surrounding few vertebrae fragments were dehydrated in ethanol, and embedded in Bioacryl hydrophilic resin for 2 days under ultraviolet light at 0–4°C (Scala et al., 1992). This resin generally preserves immunoreactivity and can be utilized for immunohistochemistry at the light and electron microscopic level (Scala et al., 1992; Alibardi, 2019a, 2020a). Tissues were sectioned with an ultramicrotome at 2–4 µm in thickness in cross-sections, collecting plastic sections of the SC every 20–

30 µm, starting from the rostral SC stump and moving toward the central transected area, the bridge, and then continuing into the caudal stump of the SC, spanning across the injured region (**Figure 1**). Sample sections were stained with 1% toluidine blues for the histological control. In areas of interest in the rostral SC stump, in the bridge region, and also in the caudal region spanning across the injured region, 60–90 nm thick sections of the entire SC were collected on nickel grids for the immunogold cytochemical study under the electron microscope.

Western blot assay

The brains from the sacrificed lizards were rapidly removed from the skull and immersed in an extractive solution for proteins. Tissues were homogenized in 8 M urea/50 mM Tris-HCl at pH 7.6 containing 0.1 M 2-mercaptoethanol/1 mM dithiothreithol/and 1% protease inhibitor (Sigma, St. Louis, MO, USA). The particulate matter was removed by centrifugation at 10,000 × *g* for 5 minutes, and protein concentration was assayed by the Bradford method before electrophoresis. The latter was conducted after loading 70 µg of protein on each lane of the electrophoretic gel (12% sodium dodecyl sulfate-polyacrylamide gels, SDS-PAGE). Proteins were separated using the MiniProtean III electrophoresis apparatus (Bio-Rad, Hercules, CA, USA). For western blotting, the proteins separated in SDS-PAGE were transferred to nitrocellulose paper. After western blotting, membranes were stained with Ponceau red to verify the protein transfer and incubated with a primary anti-mouse antibody for GAP-43 or an anti-rabbit antibody for nerurofilament-200 (see below). In controls, the primary antibody was omitted. After extensive rinsing, the nitrocellulose strip was incubated with secondary FITC-conjugated antibodies (anti-mouse or anti-rabbit) diluted 1:2000 for 1 hour. Detection was performed using the enhanced chemiluminescence procedure developed by Amersham (ECL, Plex Western Blotting System, GE Healthcare, UK).

Light and electron microscopy immunocytochemistry

The plastic sections for light microscopy immunofluorescence were initially incubated in 0.5 M citrate buffer at pH 5.6 in a microwave oven for 5 minutes and rinsed in distilled water. The sections were immersed in 0.05 M Tris buffer at pH 7.6, containing 3% bovine serum albumin (BSA), and pre-incubated for 30 minutes in 5% Tris buffer containing 5% normal goat serum (NGS) to block non-specific antigenic epitopes. The sections were incubated for 6 hours at room temperature with different antibodies. A mouse monoclonal antibody (G-9264 from Sigma) was utilized to detect GAP-43 (or neuroregulin), a marker of axonal growth cones and nerve cells. For neurofilament detection, a rabbit polyclonal antibody was utilized (N-4142, Sigma). The antibodies were diluted 1:80 in the Tris Buffer and applied on the sections while in control sections the primary antibody was omitted from the incubation solution. After repeated rinses in buffer, the sections were incubated with goat anti-mouse or anti-rabbit secondary antibodies conjugated to fluorescein isothyocyanate (FITC, Sigma, producing a green fluorescence) or tetramethyl rhodamine iso-thiocyanate (TRITC, Sigma, producing a red fluorescence), mounted in anti-fading Fluoromount (Sigma), and observed under a fluorescent microscope. Some sections were counterstained for the nuclei using 4',6-diamidino-2-phenylindole (DAPI; 1: 1000 dilution in buffer) for 10 minutes at room temperature in the dark. The sections were studied under a fluorescence microscope, and images were recorded by a digital camera and imported into a computer for making figure plates using the program Photoshop version 8.0 (Adobe Systems Inc., San Jose, CA, USA).

For immunogold detection under an electron microscope, sections on Nickel grids were incubated for 4 hours at room temperature in the mouse GAP-43 antibody diluted 1:80 in 0.05 M TRIS-HCl buffer at pH 7.6 containing 1% Cold Water Fish Gelatin. In negative controls, the primary antibody was omitted. After the incubation period, the sections were rinsed in buffer and incubated for 1 hour at room temperature with goat anti-mouse Gold-conjugated secondary antibody (Sigma, 10 nm gold particles). Some grids went through a silver enhancement procedure developed by British Biocell International (BBB, Bristol, UK) to increase the size of gold particles and allow the detection of labeled cells/structures at lower magnification. The suggested intensification method followed the manufacturer instructions (BBI, SEKB250) with intensification periods of 6–7 minutes. Finally, the grids were rinsed in the buffer, dried and stained for 4 minutes with 2% uranyl acetate, and then observed under an electron microscope at 60 kV (Zeiss 10C/CR).

Two samples were utilized to display the histology and ultrastructure of the regenerated lumbar SC at 29 days post-transection according to previous studies (Alibardi, 2014a, b; **Figure 1A**). The tissues were fixed in 2.5% of glutaraldehyde, post-fixed in 2% osmium tetroxide, dehydrated in ethanol, and embedded in Epon resin.

Results

Behavioral observations

The injured lizards at 11, 19 and 22 days after SC injury were paralyzed, dragging their stiff hindlimbs as they moved using only the forelimbs. However, at 34 days 2 out of the 3 lizards analyzed could move the hindlimbs for walking and running. The third lizard moved well only one limb but the other (right) was still rigid and slowly moving. The three lizards analyzed after 3 months from injury utilized the hindlimbs for stepping and running with different abilities but one animal could not move well the right hindlimb. However, the animals at 34 days and 3 months post-injury could not uplift their body using the hindlimbs when lining on a wall, evidencing lack of strength for jerking.

Histological and electron microscopy observations

The analysis of the transected SC at 22 and 34 days showed that at the time of transection, a bridge region (**Figure 1A–A3**) formed, which was composed of a tissue containing nervous fibers mixed to connective fibers derived from the meninges. The cross sections collected from the rostral SC stump (**Figures 1A4–A5** and **2A**) that moved into the bridge (**Figures 1A5–A6** and **2B–G**) and finally into the caudal SC stump (**Figure 1A6–A8**) showed that the injured SC changed in both diameter and structure. Initially, the injured SC gradually lost the demarcation between grey and white matter, the central canal enlarged into a dilated ependymal ampulla, while in the central area of the bridge, the ependymal canal disappeared leaving a glial and connective mass of tissue among empty spaces. The latter was likely derived from degenerated myelinated axons and nerve cells (**Figure 2B–G**). Some nerve bundles, resembling regenerating nerves, were also observed in the central regions of the bridge, suggesting regeneration at 22-34 days (**Figure 2G**).

In recovered SC at 34 days post-injury, the electron microscope showed presence of numerous cavities formed

among sparse cells, most of which appeared as electron-dense oligodendrocytes, sometimes detected in course of initial myelination of sparse axons (**Figure 2H–J**). The cytoplasm of these cells, like that surrounding the myelinating axons, appeared more electron dense than the cytoplasm of neurons and astroglial cells. Other sparse cells present in the bridge were electron-pale in the cytoplasm and the nucleus was also pale although numerous heterochromatic zones were present (**Figure 2K**). The latter cells were recognized as astrocytes because of their content in intermediate filaments that often formed intracellular bundles inside cytoplasmic protrusions.

Western blot assay results

The immunodetection of labeled proteins extracted from the brain showed a prevalent band at 48–50 kDa, and other minor bands around 90, 42, 35 and 17 kDa (first lane on the left in **Figure 3**). A main and broad band at 200–240 kDa was instead reactive for NF200 (second-central lane in **Figure 3**). Controls, omitting the primary antibody, did not show bands (last lane on the right in **Figure 3**).

Immunofluorescence for GAP-43

After 11 days, the proximal stump of the SC (**Figure 1A5**) showed numerous degenerating axons in the grey matter of the proximal stump. SC become thinner when it moved into the bridge and consisted of a degenerating nervous tissue where no neurons were visible around the enlarged ependymal ampulla (**Figures 1A5** and **4A–D**). Numerous neurons, including motor neurons of the proximal SC stump at 11–22 days showed a cytoplasmic granular immunolabeling for GAP-43 (**Figures 1A5** and **4E**). Numerous GAP-43 labeled axons were also seen in the proximal region of the bridge (**Figure 1A5**) at 11, 19 and 22 days, but they were un-evenly distributed in the degenerated SC (**Figure 4G–J**). Although a quantitative analysis was not done in the central region of the bridge observed in cross-section, devoid of ependyma (**Figure 1A6**), a number of GAP-43 positive axons with variable labeling intensity were observed, and those more intensely labeled varied from 10 to 30 in the available cases. The labeling was not uniform on the entire SC section but it was only present in external areas, corresponding to the white matter, with respect to the dilated ependymal ampulla where it was present (**Figure 1A5** and **A7**), and in sparse areas of the central bridge where the ependyma was missing. Control sections were unlabeled (**Figure 4K**). Few GAP-43-labeled axons were also seen in the distal stump of the SC (**Figure 1A7**; not shown).

The single DAPI staining of cross-sectioned SC evidenced that more numerous cells were present around the enlarged ependymal ampullae in the bridge at 19, 22 and 34 days after injury in comparison to those present around the central canal in the proximal stump of the SC, as a result of the intense cell proliferation in the bridge (**Figures 1A5–A7**, **5A** and **B**). The double immunostaining, for DAPI and GAP-43, confirmed that few intensely labeled axons (10–30/section) were present in the bridge regions lateral to and around the ependymal canal. In more central regions of the bridge, other labeled axons appeared irregularly distributed within the mass of the bridge tissue where the ependymal canal was missing (**Figures 1A5** and **5C–E**).

Immunogold labeling for GAP-43 at 22 days post-injury

To support immunofluorescence observation, some sections at 22 days of SC regeneration were also analyzed under immunogold labeling and immunogold with silver intensification to detect cell and axonal profiles (**Figures 6** and **7**) within the proximal regions of the bridge region (levels corresponding to A5–A6 in **Figure 1**). Immunogold labeling using gold particles of 10 nm in diameter showed immunolabeling details at high magnification. Using the silver enhancement procedure to enlarge gold particles it was possible to detect labeling at lower magnification of different cells and neuropilar elements. The survey was made scanning entire thin cross-sections of the bridge region under the electron microscope at high magnification (15000–40000 fold magnification for immunogold; 2000–5000 fold magnification after silver enhancement), and this procedure allowed the detection of few sparse labeled cells and axonal profiles (**Figure 6A–C**). Immunogold-labeled cytoplasmic regions of likely nerve cells or small axons were labeled but the limited ultrastructural preservation did not allow the safe detection of growth cones storing numerous synaptic vesicles and neuro-filaments or neurotubules (**Figure 6A–C**). Control sections, however, did not present any gold labeling (**Figure 6D**).

Labeled cells and axons, including growth cones containing round or pleomorphic synaptic vesicles, were analyzed on sections labeled using immunogold. Other sections were used for studies after silver intensification. The latter method allowed detecting labeled structures at low magnification (**Figure 6E** and **F**). However, labeled axons were occasionally seen in the central region of the bridge at 22 days post-injury while they became more common near the proximal SC stump. Immunofluorescence staining (**Figure 4E**) revealed that the cytoplasm of various smaller and larger neurons present in the proximal stump and in the initial bridge region (indicated in **Figure 1A4** and **A5**) was immunoreactive for GAP-43 (**Figure 7A** and **B**). Compared with glial cells, all these labeled cells were identified as roundish-oval shaped large- or medium-sized neurons with pale and euchromatic nuclei. Control sections were instead unlabeled or showed a low and random and un-patterned distribution of few irregular particles (**Figure 7C**).

Neurofilament-200 immunofluorescence

The immunolabeling of cross-sectioned bridge regions close to the proximal stump showed numerous intensely labeled axons in the external areas of the bridge, occupied by white matter at 19–22 days post-amputation (**Figures 1A5** and **8A–C**). Blood vessels exhibited a non-specific autofluorescence, yellowish for FITC and pinkish for TRITC (**Figure 8A**). Labeled axons were also noted around the dilated ependymal ampullae in cross sections of the bridge at 34 days post-injury, and some axons or collateral sprouting, were also noted among ependymal cells (**Figure 8D**). The number of immunolabeled axons or axonal sprouting increased dramatically in the bridge of lizards at 3 months after injury, in the white matter of the bridge and few were also observed around the still dilated ependymal ampullae (**Figure 8E** and **F**). This was confirmed by double labeling staining that evidenced the higher density of cells present in the bridge at 11–22 days post-injury and the sparse but numerous axons present in peripheral and peri-ependymal regions of the bridge (**Figure 9A** and **B**). Although no quantification was done, the labeled axons appeared to increase at 34 days and 3 months-post-injury (**Figure 9C**). Finally, no labeling for NF200 was seen in control sections of the bridge (**Figure 9D**).

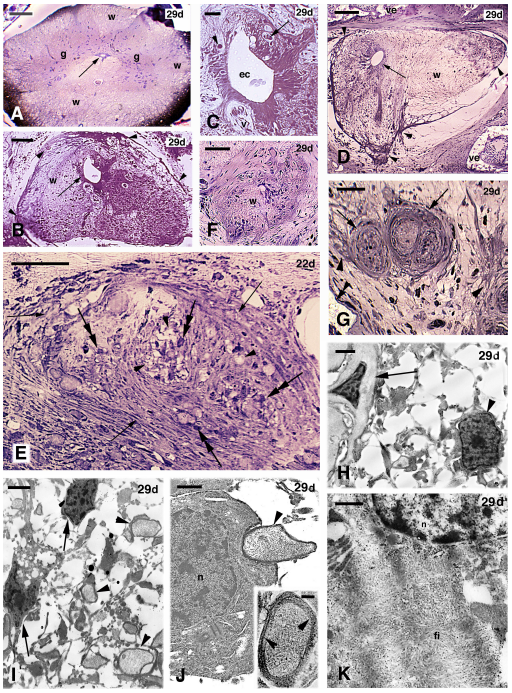

Figure 2 | Histology (A–G, toluidine blue stain) and electron microscopy (H–K) of representative cross-sectioned regions of the regenerating SC at 22 days (E) and 29 days (A–D, F–K) post-injury.
(A) Cross-section of lumbar SC at about 0.5 mm from the bridge showing H-shaped grey matter and sparse pale areas of degenerating axons in the white matter. The arrow indicates the normal ependymal canal. (B) Initial bridge region (level A4–A5 in Figure 1) showing size reduction, degeneration and disorganization in the white and grey matter, and dilatation of the ependymal canal (arrow). Arrowheads point to meningeal infiltration. (C) Detail of the dilated ependymal canal with a degenerating cell (arrow) and a lymphocyte or pycnotic cell (arrowhead). (D) Residual SC with enlarged central canal (arrow) in a region toward the mid bridge (levels A5–A6 in Figure 1). The meninges penetration has occurred in different areas (arrowheads). (E) Central bridge tissue formed by a mix of degenerating myelin axons (arrowheads), fibrocytes (arrows), and sparse nuclei of glial cells (double arrows). (F) Caudal region of the bridge (level A5–A6 in Figure 1) where a narrow white matter fascicle, made of glial cells and pale areas (axons/glial elongation), is present. (G) Detail on other caudal bridge area (level A5–A6) where only two nervous bundles (arrows) surrounded by scarring connective and meningeal cells (arrowheads) have remained. The double arrowhead indicates vertebral bone. (H) A likely oligodendrocyte (arrowhead) and astrocyte (arrow) seen in central vacuolated bridge tissue. (I) Some myelinating axons near likely oligodendrocytes (arrows) are seen in vacuolated central bridge tissue. Arrowheads indicate myelinated axons. (J) Detail on a myelinating axon (arrowhead) that is adherent to the electron-dense cytoplasm of an aligodendrocyte. Inset shows the myelinating cytoplasm (arrowheads). (K) Likely astrocyte with pale cytoplasm containing numerous intermediate filaments. e: Ependyma; ec: ependymal (central) canal; fi: glial filaments; g: grey matter; n: nucleus; v: blood vessel; ve: vertebral bone; w: white matter. Scale bars: 100 µm in A, 50 µm in B, D, E, F, 10 µm in C, 20 µm in G, 2 µm in H and I, 1 µm in J, 0.2 µm in inset of J, 0.5 µm in K.

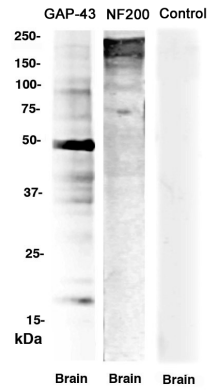

Figure 3 | Western blotting results from brain extracts for GAP-43 and NF200.
GAP-43: Growth associated protein 43.

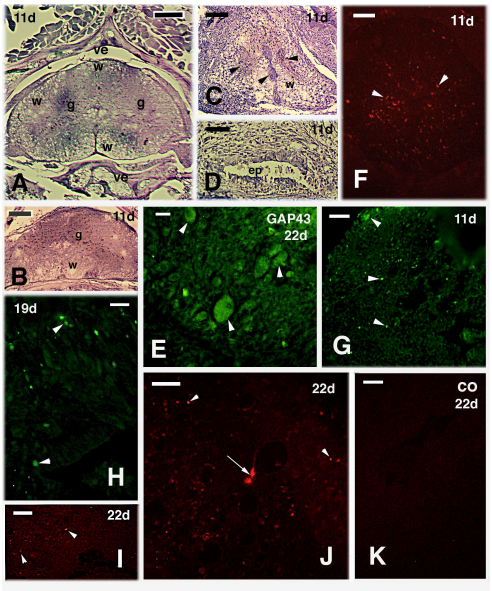

Figure 4 | Histology (A–D, toluidine blue stain) and immunofluorescence for GAP-43 (E–K) of regenerating SC within ~3 weeks after injury (11, 19 and 22 days post-injury).
(A) Numerous vacuolated areas derived from axonal degeneration are seen in the white matter of this cross-sectioned SC located near the bridge (level A4–A5 in Figure 1). (B) In this section near the bridge, no distinction between grey and white matter is evident. Scale bar: 100 µm. (C) Initial segment of the bridge (level A4–A5 in Figure 1) showing fragments of grey matter (arrowheads) surrounded by most degenerating white matter. (D) Detail on an enlarged ependymal canal present in the bridge (level as in Figure 1A5). (E) Immunofluorescent neurons (arrowheads) in the grey matter of proximal SC stump (level A5–A6 in Figure 1). (F) Labeled axons (arrowheads) in central bridge tissue (level A5–A6 in Figure 1). (G) Labeled axons (arrowheads) in peripheral area of the bridge (level A6 in Figure 1). (H) Another area of the central bridge (level A6–A7 in Figure 1). Arrowheads indicate the grey matter. (I) Peripheral area of the bridge with sparse labeled axons (arrowheads; level A6–A7 in Figure 1). (J) Central area of the bridge with sparse labeled axons (arrowheads; level A5–A6 in Figure 1). The arrow indicates a possible immunoreactive cell (neuron or growth cone?). (K) Immune-negative area of the bridge (level A5–A6 in Figure 1). Scale bars: 100 µm in A–C; 20 µm in D, 10 µm in E–K. ep: ependymal canal; GAP-43: growth associated protein 43; g: grey matter; SC: spinal cord; ve: vertebral bone/neural arch; w: white matter.

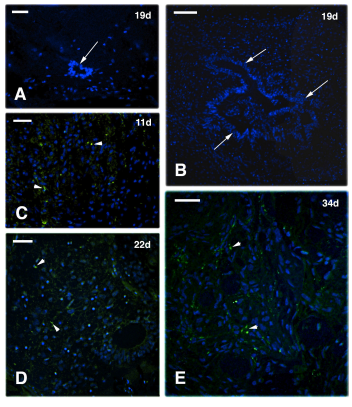

Figure 5 | DAPI-nuclear fluorescence (blue; A and B) and double labeling (DAPI blue and GAP43 green C–E) at different days post-injury (11–34 days).
(A) Section in the initial bridge with small central canal (arrow; level A4–A5 in Figure 1). Scale bar: 10 µm. (B) Enlarged irregular ependymal canal (indicated by arrows) in the central area of level A5 (Figure 1). Scale bar: 20 µm. (C) Sparse immunolabeled axons (arrowheads) observed in central bridge (level A5–A6 in Figure 1). Scale bar: 10 µm. (D) Few labeled axons (arrowheads) are seen in central area of the bridge (level A5–A6 in Figure 1). Scale bar: 10 µm. (E) Sparse labeled axons (arrowheads) are still seen in the bridge (level A5–A6 in Figure 1) after more than 1 month post-injury. Scale bar: 10 µm in A, C–E, 20 µm in B. DAPI: 4′,6-Diamidino-2-phenylindole.

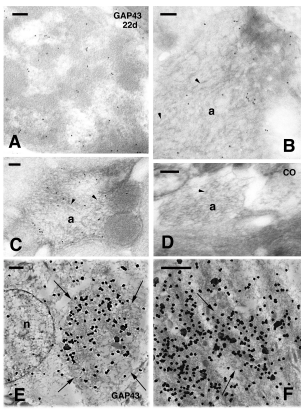

Figure 6 | Immunogold (A–D) and immunogold with silver intensification (E and F) for growth associated protein 43 (GAP-43) detected at the beginning of the bridge area (level A5 in Figure 1) in injured SC at 22 days post-injury.
(A) Diffuse labeling in a cytoplasmic profile located among the white matter. (B) Diffuse labeling in a likely axonal tract containing cytoskeletal filaments (a). Arrowheads indicate likely microtubules. (C) Other small axonal region (a) containing microtubules (arrowheads) and intermediate filaments. (D) Immunonegative control section containing a small axonal profile (a). The arrowhead indicates cytoskeletal filaments. (E) Immunolabeled axonal section (arrows) close to an immunonegative glial cell (n, nucleus). (F) Close-up to a labeled axonal section (growth cone?) containing synaptic vesicles (arrows). Scale bars: 100 nm in A–C, 200 nm in D, 0.5 µm in E.

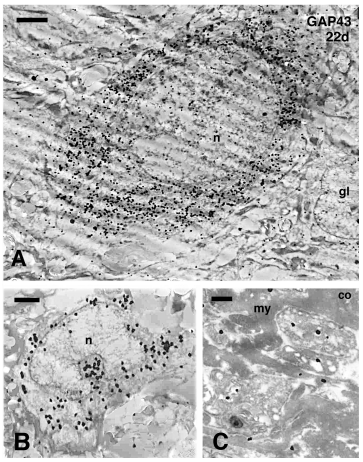

Figure 7 | Immunogold with silver intensification labeling for growth associated protein 43 in nervous areas of the bridge around the dilated ependymal canal (level A5 in Figure 1) in injured spinal cord at 22 days post-injury.
(A) Neuron with intensely labeled cytoplasm (n, nucleus) located near an immunonegative glial cell (gl). (B) Small neuron with labeled cytoplasm (n, nucleus). (C) Immunonegative control section (co); my: myelin. Scale bars: 1 µm in A and B, 0.5 µm in C.

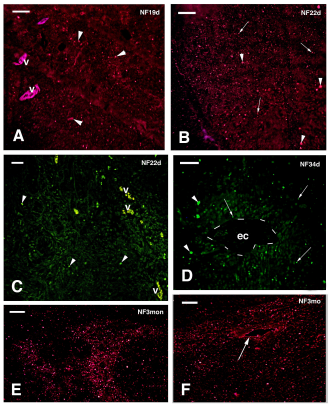

Figure 8 | Immunofluorescence for NF200 in cross sections of the bridge at 19, 22, 34 days and 3 months post-injury (levels A5–A7 in Figure 1).
(A) Central region of the bridge with labeled axons (arrowheads). Blood vessels containing erythrocytes (v) fluoresce non-specifically. (B) Peripheral region of the bridge with numerous small (arrows) and larger (arrowheads) labeled axons. (C) Central area of the bridge showing sparse labeled axons (arrowheads). Blood vessels (v) autofluoresce in their erythrocytes. (D) Detail of enlarged ependymal canal (ec, outlined by dashes) with surrounding larger (arrowheads) and thinner (arrows) axons. (E) Numerous axons with uneven distribution are seen in this peripheral region of the central bridge (level A6) after over 1 month from the injury (a lizard with a good recovery of limb movements). (F) Many labeled axons are seen in this central region of the bridge (level A5 in Figure 1), surrounding the dilated central canal (arrow). Scale bars: 10 µm in A–D, 20 µm in E and F.

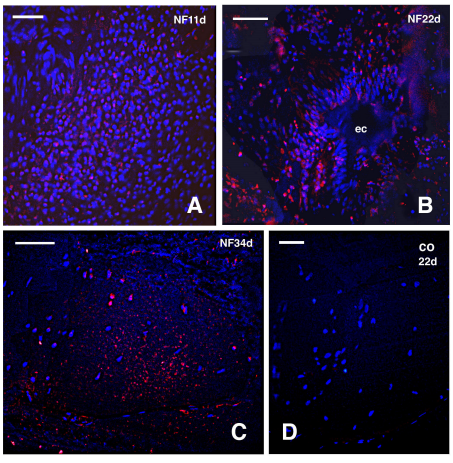

Figure 9 | Blue nuclear fluorescence (DAPI) and red immunofluorescence (TRITC) for NF200 observed in the bridge at 11, 22, 34 days post-injury (levels A5–A6 in Figure 1).
(A) Numerous axons appearing as dots are seen in this area at 11 days. (B) Central region of the bridge with dilated ependymal canal (ec) showing numerous axons present around it. (C) A large number of axons appearing as dots are labeled in the central bridge at more than 1 month post-injury. (D) Immunonegative control. Scale bars: 10 µm in A, B, D, 20 µm in C. DAPI: 4′,6-Diamidino-2-phenylindole; TRITC: tetramethyl rhodamine iso-thiocyanate.

Discussion

Presence of regenerating axons in the recovering lumbar SC of lizards

The bioinformatics data support a cross-reactivity of the employed anti-GAP-43 antibody with a lizard GAP-43. The present western blot analysis shows that a GAP-43-like protein is detected around 48 kDa, a slightly higher molecular weight than the mammalian protein. A neurofilament protein of 200–240 kDa is also immunoreactive for the employed antibody. These western blot results indicate that these two proteins are present in the nervous system of the lizard, supporting the bio-informatic and the immunohistochemical observations. However, GAP-43 immunoreactive axons are much less frequent that those labeled for NF200, reflecting the fact that few regenerating axons are present in the bridge, as previously indicated by a tract tracing study (Alibardi, 2014a). The study using GAP-43, a marker of growth cones and axonogenesis in different areas of the normal and regenerating nervous tissues (Woolf et al., 1990; Curtis et al., 1993; Kapfhammer and Schwab, 1994; Rodger et al., 2001), has shown a variable but however limited number of immunopositive axons present in the bridge region, 10–30, confirming previous histological and tract-tracing studies (Alibardi, 2014a, b). While growing axons are numerous in the proximal stumps they become few or rare in the bridge, depending on the cases analyzed.

The intense labeling for GAP-43 observed in some neurons of the proximal stump of the SC suggests that this protein fabricated in the neuronal cytoplasm is anterogradely transported into the growing axonal cones during sprouting or regeneration (Woolf et al., 1990). These axons, including those possibly regenerating, are seen irregularly distributed within the initial regions of the bridge where the ependymal ampullae are still present. However, the number of GAP-43 labeled axons dramatically decreases in the central region of the bridge where no ependymal epithelium is present. This suggests that a local axonal sprouting is present in the proximal region of the transected SC while very few axons really can cross the bridge region and re-establish SC connections between the proximal and distal SC stumps. Among these reconnecting axons, some may represent those generated from the small neurons of the intrinsic spinal locomotor system (Miller and Scott, 1977; Alibardi, 2014a). The higher number of NF200 labeled axons observed in the present study in comparison to those labeled for GAP-43 further supports the idea that axonal sprouting is present in the initial, proximal segment of the SC entering the bridge area. Taken a previous tract-tracing study together, the present results indicate that only few axons can cross the gap (bridge) and re-connect with the caudal stump of the SC. Despite this limited axonal regeneration, some neural circuits are probably reactivated and may participate in the formation of these motor circuits, as indicated by studies on the regeneration of fish SC (Miller and Scott, 1977; Rasmussen and Sagasti, 2016).

Limitation of lumbar SC regeneration in lizards compared to anamniotes

The present qualitative study extends previous information on the ability to recover some hindlimb movements after the initial paralysis in lizards (Srivastava, 1992; Srivastava et al., 1994; Alibardi, 2014a, b). The comparative analysis on the ability to recover in ecthotherm amniotes, the reptiles, can provide further information on the evolution of the complete or partial inability of nerve regeneration in the central nervous system of mammals (Tanaka and Ferretti,

2009; Lee-Liu et al., 2013). Among terrestrial vertebrates, lizards are the only amniotes capable to regenerate an organ, the tail with a simplified SC (Gilbert and Vickaryus, 2018; Alibardi, 2019b, 2020b). These studies have indicated that to regenerate an organ, including the SC, the post-traumatic reparative process must re-create embryonic-like conditions that mimic the environment of growing nerves during development. This includes the production of an immune-suppressive and healing immune-cells and hyaluronate-rich environment that allows for axonal regeneration, like in the regenerating tail, studies are presently active. The limited but however important SC regeneration in lizards (and turtles, see Reherman et al., 2009, 2011) is aimed to discover which factors and molecules are activated during this recovering to be compared with endotherm amniotes.

The few studies so far carried out on lizards have reported that 1–2 weeks after transection, the animals show a rigid paralysis where lizards slowly drag the hindlimbs that cannot be extend or retracted. At 2–3 weeks post-injury, a flaccid paralysis is present where lizards move-undulate their back and start moving the hindlimbs in some individuals, apparently regaining full flexion and extension of the hindlimbs at 4 weeks and 3 months post-amputation. At this late time, some lizards can also run and are able to turn around when laid on the back, but they cannot lift the body by the hindlimbs to climb vertical surfaces. Apparently this functional recovery has not been described in the lizard Anolis carolinensis after thoracic or lumbar lesions (Simpson and Duffy, 1994). Previous studies indicated that gliogenesis is present in the lumbar SC of lizards while rare neurons are formed in the dilated ependymal epithelium present in the proximal area of the bridge (Alibardi, 2014a, b, c). Cell proliferation occurs in the ependyma initially entering the bridge region and from astroglial and oligodendroglia cells present in the bridge area that behave as stem/progenitor elements (Alibardi, 2019a). Although expressing NOGO-A, both oligodendrocytes and axons appear to regenerate in the transected SC of lizards (Alibardi, 2020a). Also connective cells (fibrocytes) of the scar component of the bridge derive from the surrounding, damaged meninges that also may host stem/progenitor cells that invade the damaged SC, contributing to the formation of the bridge tissue. Also in freshwater turtles (Trachemys dorbignyi) after SC transection and paralysis, the recovery of limb movement and swimming is high. Notwithstanding, these movements are not like the original ones showing slow and poorly coordinated limb movements in comparison to the original coordination (Reherman et al., 2009, 2011).

Reptilian regeneration of the SC therefore appears slightly better than in mammals, but still very limited when compared to SC regeneration in anamniotes. In fish and amphibians, the transection of the SC is followed by more completed both anatomically, (grey and white matter are variably re-formed), and physiologically (recovering of movements after the initial paralysis) (Davis et al., 1989, 1990; Rasmussen and Sagasti, 2016). However, also the SC in newts regenerates with a simpler anatomical organization with respect to the pre-trauma condition (Davis et al., 1989). This, however, does not impair the functionality of the SC and both motor and sensory coordination are well recovered but not with the same performance as in the original SC (Davis et al., 1990). In the interesting case of anurans, while regeneration of the SC occurs in the first stage of tadpole development, the capability to form neurons, regenerating axons and to recover the interruption of the SC after transection lowers to disappear after metamorphosis, when adult frogs become fully terrestrial (Filoni et al., 1984; Beattie et al., 1990; Chernoff, 1996; Ferretti et al., 2003; Lee-Liu et al., 2013). This event leads to a permanent paralysis also in frogs or toads after SC injury, and one of the main negative causes to block SC regeneration seems to be linked to the formation of a glial scar and to the increased efficiency of the immune system after metamorphosis (Mescher et al., 2016).

In conclusion, the present study indicates that a broad axonal regeneration and sprouting occurs in the proximal SC stump of lizards, as suggested by the NF200 antibody. In contrast, few GAP-43-positive axons regenerate through the bridge formed after lumbar SC transection. These few axons, however, likely contribute to the reactivation of the limited but significant recovery of hindlimb movements that occurs at about 1 month after the injury in numerous lizards after their initial paralysis. The study on the microenvironment generated in the injured SC of lizards (and turtles) may indicate whether similar permissive conditions can be induced in endotherm amniotes for the growth of axons through the interrupted SC.

Acknowledgments: *Research almost completely supported by Comparative Histolab Padova. Dr. Francesca Borsetti (Proteome Service, Dipartimento di Biologia, Università di Bologna) ran the electrophoresis and WB.*
Author contributions: *Concept, design, funding, experiments, study analysis, paper writing: LA. LA approved the final version of the paper.*
Conflicts of interest: *None declared.*
Financial support: *None.*
Institutional review board statement: *The surgical procedures utilized in the study followed the regulations on animal care and experimental procedures under the Italian Guidelines (art. 5, DL 116/92).*
Copyright license agreement: *The Copyright License Agreement has been signed by the author before publication.*
Data sharing statement: *Datasets analyzed during the current study are available from the corresponding author on reasonable request.*
Plagiarism check: *Checked twice by iThenticate.*
Peer review: *Externally peer reviewed.*

References

Alibardi L (2014a) Observations on lumbar spinal cord recovery after lesion in lizards indicates regeneration of a cellular and fibrous bridge reconnecting the injured cord. J Dev Biol 2:210-229.

Alibardi L (2014b) Ultrastructural observations on lumbar spinal cord recovery after lesion in lizard indicates axonal regeneration and neurogenesis. Int J Biol 7:122-136.

Alibardi L (2014c) Histochemical, biochemical and cell biological aspects of tail regeneration in lizard, an amniote model for studies on tissue regeneration. Progr Histoch Cytoch 48:143-244.

Alibardi L (2019a) Observations on the recovering lumbar spinal cord of lizards show multiple origins of the cells forming the bridge region including immune cells. J Morphol 281:95-109.

Alibardi L (2019b) Review: Cerebro Spinal Fluid Contacting Neurons (CSFCNs) in the regenerating spinal cord of lizards and amphibians are likely mechanoreceptors. J Morphol 280:1292-1308.

Alibardi L (2020a) NOGO-A immunolabeling is present in glial cells and some neurons of the recovering lumbar spinal cord in lizards. J Morphol 281:1260-1270.

Alibardi L (2020b) Appendage regeneration in anamniotes utilizes genes active during larval-metamorphic stages that have been lost or altered in amniotes: the case for studying lizard tail regeneration. J Morphol 281: 1358-1381.

Beattie MS, Bresnahan JC, Lopatet G, Lopate G (1990) Metamorphosis alters the response to spinal cord transection in Xenopus laevis frogs. J Neurobiol 21:1108-1122.

Berry M, Riches AC (1974) An immunological approach to regeneration in the central nervous system. Br Med Bull 30:135-140.

Chernoff EA (1996) Spinal cord regeneration: a phenomenon unique to urodeles? Int J Dev Biol 40:823-831.

Clearwaters KP (1954) Regeneration of the spinal cord of the chick. J Comp Neurol 101:319-329.

Curtis R, Green D, Lindsay RM, Wilkins GP (1993) Up-regulation of GAP43 and growth of axons in rat spinal cord after compression injury. J Neurocyt 22:51-64.

Davis BM, Duffy MT, Simpson SB (1989) Bulbospinal and intraspinal connections in normal and regenerated salamander spinal cord. Exp Neurol 103:41-51.

Davis BM, Ayers JKL, Koran L, Carlson J, Anderson M, Simpson SB (1990) Time course of salamander spinal cord regeneration and recovery of swimming: HRP retrograde pathway tracing and kinematic analysis. Exp Neurol 108:198-213.

Ferretti P, Zhang F, O'Neil P (2003) Changes in spinal cord regenerative ability through phylogenesis and development: lessons to be learnt. Dev Dyn 226:245-256.

Filoni S, Bosco L, Cioni C (1984) Reconstitution of the spinal cord after ablation in larval Xenopus laevis. Acta Embryol Morphol Exp 5:109-129.

Gadani SP, Walsh JT, Lukens JR, Kipnis J (2015) Dealing with danger in the CNS: response of the immune system to injury. Neuron 87:47-62.

Gilbert EAB, Vickaryous MK (2018) Neural stem/progenitor cells are activated during tail regeneration in the leopard gecko (Eublepharis macularius). J Comp Neurol 526:285-309.

Kapfhammer JP, Schwab ME (1994) Inverse patterns of myelination and GAP-43 expression in the adult CNS: neurite growth inhibitors as regulators of neuronal plasticity? J Comp Neurol 340:194-206.

Lauro GM, Margotta V, Venturini G, Techner A, Caronti B, Palladini G (1992) Correlation between immune response and CNS regeneration in vertebrate phylogenesis. Boll Zool 59:215-220.

Lee-Liu D, Edwards-Faret G, Tapia VS, Larraín J (2013) Spinal cord regeneration: lessons for mammals from non-mammalian vertebrates. Genesis 51:529-544.

Lennon VA (1994) Cross-talk between nervous and immune systems in response to injury. Prog Brain Res 103:289-292.

Martin GF, Terman JR, Wang XM (2000) Regeneration of descending spinal axons after transection of the thoracic spinal cord during early development in the North American opossum, Didelphis virginiana. Brain Res Bull 53: 677-687.

McDonough A, Martínez-Cerdeño V (2012) Endogenous proliferation after spinal cord injury in animal models. Stem Cells Int 2012:387513.

Mescher AL, Neff AW, King MW (2016) Inflammation and immunity in organ regeneration. Dev Comp Immunol 66:98-110.

Miller S, Scott PD (1977) The spinal locomotor generator. Exp Brain Res 30:387-403.

Nicholls J, Saunders N (1996) Regeneration of immature mammalian spinal cord after injury. Trends Neurosci 19:229-234.

Raffaelli E, Palladini G (1969) Rigenerazione delle cellule nervose e degli assoni del midollo spinale dorsal di Lacerta sicula. Boll Zool 36:105-110.

Rasmussen JP, Sagasti A (2016) Learning to swim again: axon regeneration in fish. Exp Neurol 287:318-330.

Reherman MI, Marichal N, Russo R (2009) Neural reconnection in the transected spinal cord of the freshwater turtle Trachemys dorbignyi. J Comp Neurol 515:197-214.

Rehermann MI, Santiñaque FF, López-Carro B, Russo RE, Trujillo-Cenóz O (2011) Cell proliferation and cytoarchitectural remodeling during spinal cord reconnection in the fresh-water turtle Trachemys dorbignyi. Cell Tissue Res 344:415-433.

Rodger J, Bartlett CA, Harman AM, Thomas C, Beazley LD, Dunlop SA (2001) Evidence that regenerating optic axons maintain long-term growth in the lizard Ctenophorus ornatus: growth-associated protein-43 and gefiltin expression. Neuroscience 102:647-654.

Scala C, Cenacchi G, Ferrari C, Pasquinelli G, Preda P, Manara GC (1992) A new acrylic resin formulation: a useful tool for histological, ultrastructural, and immunocytochemical investigations. J Histochem Cytochem 40:1799-1804.

Simpson SB Jr, Duffy MT (1994) The lizard spinal cord: a model system for the study of spinal cord injury and repair. Prog Brain Res 103:229-241.

Srivastava VK (1992) Functional recovery following reptilean (Calotus calotus) spinal cord transection. Indian J Physiol Pharmacol 36:193-196.

Srivastava VK, Maheshwari V, Tyagi SP, Ali S (1994) Histological changes in reptilean spinal cord transection: correlation with functional recovery. Indian J Physiol Pharmacol 38:189-192.

Steeves JD, Keirstead HS, Ethell DW, Hasan SJ, Muir GD, Pataky DM, McBride CB, Petrausch B, Zwimpfer TJ (1994) Permissive and restrictive periods for brainstem-spinal regeneration in the chick. Prog Brain Res 103:243-262.

Tanaka EM, Ferretti P (2009) Considering the evolution of regeneration in the central nervous system. Nat Rev Neurosci 10:713-723.

Woolf CJ, Reynolds ML, Molander C, O'Brien C, Lindsay RM, Benowitz LI (1990) The growth-associated protein GAP-43 appears in dorsal root ganglion cells and in the dorsal horn of the rat spinal cord following peripheral nerve injury. Neuroscience 34:465-478.

Zhang Z, Li F, Sun T (2012) Does repair of spinal cord injury follow the evolutionary theory? Neural Regen Res 7:849-852.

C-Editors: Zhao M, Liu WJ; S-Editor: Li CH; L-Editor: Song LP; T-Editor: Jia Y